

parHSOM: A novel parallel Hierarchical Self-Organizing Map implementation

Rebekah Lane

Computer Science & Engineering
Mississippi State University
Starkville, United States
rel250@msstate.edu

Logan Cummins

Computer Science & Engineering
Mississippi State University
Starkville, United States
nlc123@msstate.edu

Andy Perkins

Computer Science & Engineering
Mississippi State University
Starkville, United States
perkins@cse.msstate.edu

George Trawick

Computer Science & Engineering
Mississippi State University
Starkville, United States
gtrawick@cse.msstate.edu

Ioana Banicescu

Computer Science & Engineering
Mississippi State University
Starkville, United States
ioana@cse.msstate.edu

Sudip Mittal

Computer Science
University of Alabama
Tuscaloosa, United States
sudip.mittal@ua.edu

Abstract—The digital age has completely transformed the way that information is processed and stored, which makes cybersecurity a crucial field of research. Cybersecurity contains many different domains, but this work focuses on Intrusion Detection Systems (IDSs). Within the literature, Hierarchical Self-Organizing Maps (HSOMs) have been used to create trustworthy, explainable, and AI-based IDSs. However, HSOMs are trained sequentially, which means that training HSOMs on large datasets is slow. This work presents a novel parallel HSOM architecture, called parHSOM. The purpose of this research is to investigate the effect that parallel computation has on the HSOM training time. parHSOM is tested on two different testbeds, four different output grid sizes, and five different cybersecurity datasets. Performance metrics collected from these experiments show that parHSOM consistently trains faster than the Sequential HSOM algorithm without any significant loss in performance. Additionally, this work provides a platform for further investigation into parallel HSOM implementations.

Index Terms—parallel, distributed, high performance, HPC, self-organizing map(s), SOM, hierarchical self-organizing map(s), HSOM

I. INTRODUCTION

The rise of the digital age has completely transformed the way information is processed and stored. Digital data provides greater availability compared to physical, but the cost of availability is an increased risk of exploitation. Protecting devices, systems, and their accompanying digital data is the priority of cybersecurity. Cybersecurity contains many different domains, but this work focuses on Intrusion Detection Systems (IDS). Cyberattacks are continuously changing, and thus, researchers are constantly studying various ways to improve IDS. Previous literature, has shown that artificial intelligence (AI) can be used to improve the quality of IDS. However, in order for AI-based IDS to be beneficial, cybersecurity analysts need to be able to trust their model’s decision making process. Explainable AI (XAI) is a field of research that explores methods for improving AI trustworthiness by providing explanations about

a model’s decision making process. Operators are then able to use these explanations to understand how the AI functions.

Self-Organizing Maps (SOMs), a type of XAI that clusters data, are commonly used to create understandable, AI-based IDSs [1]. The SOM algorithm creates a 2D graph representations of the relationships between data points, which provides explanations for why data is being clustered a particular way. However, the SOM algorithm is trained sequentially and is sensitive to initial conditions [2].

The Hierarchical Self-Organizing Map (HSOM) is an extension of the SOM that was designed to mitigate the SOM’s sensitivity to initial conditions. The HSOM provides greater clustering detail than the SOM, and it inherits the SOM’s advantages of trustworthiness and explainability. The HSOM is also trained sequentially, which quickly becomes impractical for large datasets. One solution to the slow training time of the HSOM would be to utilize parallel computation.

To the best of our knowledge, a parallel HSOM has not been implemented. Therefore, the purpose of this work is to design parHSOM, a parallel implementation of the HSOM algorithm. Parallel computation could enable the HSOM to train faster; moreover, the HSOM can be trained on more data resulting in a more robust model. This work analyzes various methods used to parallelize the SOM algorithm and uses that knowledge as a foundation for parHSOM. The purpose is to answer two important research questions:

RQ1: How can the Hierarchical Self-Organizing Map (HSOM) algorithm be parallelized?

RQ2: What is the performance of the parallel Hierarchical Self-Organizing Map (parHSOM) algorithm in comparison to the sequential HSOM algorithm?

The model proposed in this research parallelizes the HSOM training process and has been tested extensively on two different test environments, multiple different output grid sizes, and five different cybersecurity datasets that are prominent in the literature. To provide a thorough analysis of the parHSOM

performance and to provide an answer to RQ2, this work collected the following performance metrics - accuracy, precision, F1 Score, False Positive Rate (FPR), False Negative Rate (FNR), Training Time (TT), and Prediction Time (PT). Through experimentation, this work found that parHSOM consistently trains faster than the Sequential HSOM, with a maximum speed increase of 6.056 times faster than the Sequential HSOM. Furthermore, parHSOM performs similarly to the Sequential HSOM in terms of accuracy, precision, F1 score, FPR, FNR, and PT.

The layout for this work is as follows - Section II provides more detail on the SOM and HSOM and defines how this work researched different methods for parallelizing the HSOM, Section III outlines the design for parHSOM and discusses how the experiments for this research were conducted, Section IV provides the results from the experiments, Section V discusses how the experiment results relate to RQ1 and RQ2, and Section VI summarizes the findings of this research, lists limitations of this work, and provides future areas of research.

II. BACKGROUND & RELATED WORKS

A. Self-Organizing Maps (SOMs)

Self-Organizing Maps (SOMs) have been used in numerous fields of research, such as wireless networks, Internet of Things (IoT), and image processing [3], [4], [5]. The key advantage of using a SOM is that they have the ability to provide dimensionality reduction without loss of topographical information. Additionally, SOM networks are unsupervised and trained using competitive learning. Combined together, these features create an explainable AI model that is especially useful in the field of cybersecurity. The authors of [1] support this reasoning by demonstrating how SOMs can be used to create reliable, trustworthy Intrusion Detection Systems (IDS).

The architecture of the SOM network is simple, consisting of only two layers — an input layer and an output grid. It is trained using competitive learning, and thus, does not require labeled data. As data samples are fed into the SOM, the output neurons are modified to detect patterns and clusters in the training dataset [6]. The output of a SOM network can be utilized to generate two dimensional (2D) graph representations of relationships between the input samples.

B. SOM Algorithm

This section discusses the various equations involved in the SOM training process, which have been provided by the authors of [7]. The input layer of the SOM algorithm takes in data samples from the training dataset. The dataset can be represented by the following equation:

$$\mathbb{X} = \{x_0, x_1, \dots, x_{N-1}\} \quad x_i \in \mathbb{R}^P, \forall i = 0 \dots N - 1 \quad (1)$$

where x_i represents the individual dataset samples. The output grid is connected to the input layer utilizing weights, which are randomly initialized at the beginning of the training process. These connections are represented by equation 2.

$$\mathbb{W} = \{w_0, w_1, \dots, w_{M-1}\} \quad w_k \in \mathbb{R}^P, \forall k = 0 \dots M - 1$$

where $M = G_W G_H$, arranged as a $G_W \times G_H$ grid (2)

As mentioned previously, SOMs are used to cluster data. The first step is to randomly select a data sample from the training dataset. Then, the Best Matching Unit (BMU) is calculated for that sample using the following equation:

$$b_i = \operatorname{argmin}_k |x_i - w_k|_2 \quad (3)$$

The BMU specifies which neuron in the output grid is most similar to the input sample. The goal is to adjust the BMU, and its surrounding neighbors, so that it becomes more similar to the input sample. Adjusting the neurons in the output layer slowly fits the grid to our training data, which allows the clusters to form. The neighborhood function is calculated with equation 4:

$$h(b, k, t) = -\exp\left(\frac{\|r_b - r_k\|^2}{\delta(t)}\right) \quad (4)$$

The presence of the neighborhood function is what differentiates the SOM algorithm from the K-means clustering algorithm [8]. Instead of updating only one output neuron per input sample, the neighborhood function allows us to also update the neurons surrounding the BMU, albeit to a lesser degree.

Once the neighborhood function has been defined, the necessary updates for each specified weight can be calculated using equation 5:

$$w_k(t'+1) = w_k(t') + \alpha(t)h(b_i, k, t)(x_i - w_k(t')) \quad (5)$$

During the SOM training process, data samples are randomly selected, the BMU and neighborhood function are calculated, and the weights are updated until the convergence criteria, which are set by the researcher, have been met.

In the following subsection, this work will discuss the advantages and the disadvantages of the SOM.

C. Advantages and Disadvantages of the SOM Algorithm

The three main advantages of the Self-Organizing Map (SOM) that this paper focuses on are dimensionality reduction, topological preservation, and simplicity [2], [9]. Dimensionality reduction refers to the SOM property where information from a high dimensional dataset is mapped onto a 2D output grid. The output grid can then be used to generate a 2D graph. Topological preservation refers to the fact that no important information is lost during dimensionality reduction [9]. Finally, the SOM algorithm is simple and easy to understand because it is based off of the Euclidean distance equation. Combined together, these advantages result in a trustworthy and explainable AI algorithm.

However, the SOM also has disadvantages [2], and this paper focuses on two of them. First, it is trained sequentially. Thus, as the size of the training dataset is increased, so does the SOM training time. Second, the initialization variables for a SOM will affect the output of that SOM, which makes it sensitive to initial conditions.

D. Hierarchical Self-Organizing Maps (HSOMs)

The Hierarchical Self-Organizing Map (HSOM) is an extension of the SOM algorithm. It is unsupervised, uses competitive learning, and it inherits the advantages and disadvantages of the SOM. However, unlike the SOM algorithm, the HSOM completes multiple levels of clustering, which provides greater than the SOM. The HSOM was designed to mitigate some of the SOM algorithm’s sensitivity to initial conditions. It functions by training a SOM on the initial dataset. Then, it uses the resulting clusters to train a new SOM on each cluster, thereby providing more detail about the original SOM clusters. This process is repeated until training new SOMs no longer provides relevant information. The output from the HSOM algorithm is a hierarchy of clusters, where each new level supplies additional information as shown in Figure II-D.

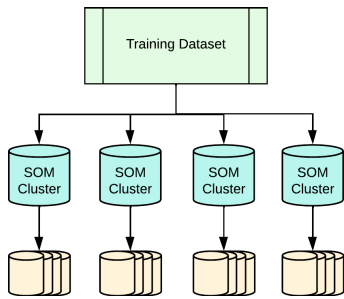


Fig. 1. A visual representation of the output from the HSOM algorithm.

As mentioned previously, the HSOM algorithm inherits dimensionality reduction, topological preservation, and simplicity from the SOM algorithm. Thus, like the SOM algorithm, the HSOM is explainable and trustworthy. However, it also inherits the SOM algorithm’s slow training time, which is compounded by the fact that the HSOM algorithm trains multiple SOMs per model.

One method for reducing the training time of the HSOM model would be to decrease the size of the training dataset. However, this could reduce the robustness of the HSOM model. Another method for reducing the training time of the HSOM model would be to use parallel computation. As a result, a literature survey was conducted to see what methods are being used to parallelize the HSOM algorithm.

E. Literature Survey

An investigation into parallel HSOM implementations within the literature returned inconclusive results, and thus, this research expanded the search to include parallelization methods for SOMs. Within the literature, SOM parallelization methods can be categorized into two main groups — those that use software optimizations to decrease the training time and those that use hardware optimizations to decrease the training time. Hardware optimizations often require special computer architectures that are not widely available. Thus, in order to produce a more accessible model, this work focused on analyzing software optimization methods.

According to the literature, software optimizations can be divided into three categories — data partitioned [3], [10], [11], [12], [7], [4], [13], [14], [15], [16], network partitioned [17], [18], [19], [20], [21], [22], [23], [8], [24], [25], [26], [27], [5], [28], [29], [30], and hybrid partitioned [31], [32]. The authors of [31] describe network partitioned methods as techniques that break up the SOM grid, while data partitioned methods are techniques that break up the dataset. Hybrid partitioned methods are a combination of data and network partitioning methods. Once either the SOM grid or the dataset is divided into separate pieces, parallel computation can commence.

The results from the survey showed a research gap surrounding parallel HSOM algorithms thus leading to RQ1 and RQ2 described in Section I. As parallel computation provides the opportunity to create more robust HSOM-based IDSs, the goal of this work was to design and evaluate a parallel HSOM.

III. DESIGN & IMPLEMENTATION

Observing the HSOM showed that it partitioned training data into independent subsets, just like the data partitioning method discussed in Section II. Thus, this work used the data partitioning method as the foundation for parHSOM. Utilizing data partitioning should decrease the training time of each layer, and thus, decrease the overall training time of the HSOM. parHSOM only parallelizes the HSOM training process. The prediction process for the HSOM algorithm remains unchanged. The DBGHSOM code from [33] was used as the basis for the Sequential HSOM and a starting point for parHSOM. Since the literature survey did not reveal any parallel HSOM implementations, this work focused on starting with the simplest HSOM implementation. Thus, DBGHSOM was reduced to its most basic HSOM components to create the baseline Sequential HSOM. Then, the Sequential HSOM was parallelized using the data-partitioned method to create parHSOM.

A. parHSOM Overview

The parHSOM is designed to be trained in two phases - an initial clustering, which is sequential, and a parallel portion. In Phase 1, a SOM is trained on the initial dataset. The resulting clusters are independent of one another. In Phase 2, a child process can be spawned for each cluster to train a SOM on that cluster, which allows this section of training to be parallelized. The CPU is responsible for assigning the child processes to different CPU processors in the most efficient manner. Increasing the number of CPU processing cores, increases the amount of resources that the CPU can assign to the children processes, and thus, should decrease the overall training time of parHSOM. This system is repeated until the finishing criteria for the HSOM are met.

B. The parHSOM Algorithm

The datasets for these experiments were preprocessed in two steps. First, the dataset is normalized using the ‘Normalizer’ function from the *sci-kit learn* python library. Then, it is split into training data and test data using the ‘train_test_split’

function from the same library. For this research, the initial dataset was split so that 80% of the initial dataset was used for the training data and 20% of the initial dataset was used for the test data. The parameters for the ‘train_test_split’ function were set so that the Sequential HSOM and parHSOM received the same training and test data for each experiment.

The first training phase of parHSOM clusters the training data provided by *Preprocessing* into independent subsets and is sequential. This is accomplished by training a SOM on the initial training data. The results from this SOM are stored in *SOM_tmp_list* for further analysis in Phase 2.

In Phase 2, the parHSOM parent process analyzes each node in *SOM_tmp_list*. If a node contains a SOM object, this means that further clustering might be necessary, and a copy of the SOM object’s information is stored in the *parent_SOM* variable. Then, the parent process spawns a child process to run the ‘Vertical Growth Function’ on *parent_SOM*. If a node does not contain a SOM object, then that signals the parent process that no further training is necessary. After a node is analyzed by the parent process, it is removed from *SOM_tmp_list* and stored in *SOM_list*, which contains all of the information for the final HSOM model. The parent process continues to analyze nodes, spawn processes, and store the nodes until *SOM_tmp_list* is empty. Once this happens, the parent process waits for all of the child processes to finish. Then, the parent process collects the results from the child processes and adds them to *SOM_tmp_list*.

Parallel Portion: This model was programmed in Python using the Python Multiprocessing library. The Multiprocessing library provides backend support that handles race conditions, prevents deadlocks, and oversees synchronization of the processes and access to resources. A Multiprocessing Manager is used by the parent and child processes to share results back and forth. The Manager oversees a shared memory dictionary that allows the child processes to send back the SOMs that they trained to the parent process.

The Vertical Growth Function (VGF) is responsible for calculating the total error of a given SOM object. The total error is then used to calculate the growth threshold criteria. Once these calculations are complete, the VGF compares the error of each neuron in the SOM to the growth threshold. If the error of a given neuron is greater than the growth threshold, then the VGF trains a SOM on that neuron’s information. If the error of a given neuron is not greater than the growth threshold, then the VGF labels that neuron, either benign or malicious, and marks the neuron as a leaf in the HSOM. After analyzing a neuron, the VGF stores the resulting information to send back to the parent process.

By detailing how the parHSOM algorithm functions, this work has shown that parHSOM provides a solution to RQ1.

C. Implementation

This work tested parHSOM on two different testing environments. Testbed 1 was an Alienware Aurora R16 computer, which has 1 socket, 24 CPU cores, and 32 logical processors, and Testbed 2 was a H100 server, which has 2 sockets, 16 CPU

Algorithm 1 Phase 2

```

1: while True do
2:   while SOM_tmp_list  $\neq$  0 do
3:     nodes  $\leftarrow$  SOM_tmp_list[0]
4:     for node  $\in$  nodes do
5:       if node == SOM object then
6:         parent_SOM  $\leftarrow$  node data
7:         Spawn child process
8:         Run vertical_growth(parent_SOM)
9:       end if
10:    end for
11:    Append SOM_tmp_list[0]  $\rightarrow$  SOM_list
12:    Pop SOM_tmp_list[0]
13:  end while
14:  Wait on child processes to finish
15:  Retrieve child_process_info
16:  SOM_tmp_list  $\leftarrow$  child_process_info
17:  if SOM_tmp_list == empty then
18:    break ▷ Training is finished
19:  end if
20: end while

```

Algorithm 2 Vertical Growth Function

```

1: Calculate the error for each neuron  $\in$  parent_SOM
2: Calculate the growth_threshold
3: for neuron  $\in$  parent_SOM do
4:   if neuron_error > growth_threshold and
     num_neuron_data_samples > SOM_GRID_SIZE
     then
5:     Train a SOM on neuron_data
6:     nodes  $\leftarrow$  SOM_info
7:   else
8:     Label neuron benign or malicious
9:     nodes  $\leftarrow$  neuron
10:  end if
11: end for
12: Return nodes

```

cores per socket, and 64 logical processors. Since different output grid sizes can vary the results of a SOM, this research tested each model on four different grid sizes - 2x2, 3x3, 4x4, and 5x5. Previous literature has used accuracy, precision, recall, F1 score, False Positive Rate (FPR), False Negative Rate (FNR), Training Time (TT), and Prediction Time (PT) to evaluate the performance of the HSOM algorithm [33]. Thus, this work used the same metrics to evaluate the success of parHSOM. Each test was conducted ten times and the average result of those tests was collected for each evaluation metric.

Five cybersecurity datasets were used to assess the efficacy of parHSOM in a variety of scenarios: CIC-IDS-2017, CIC-IDS-2018, NSL-KDD, TON_IoT, and UNSW-NB15. These datasets were selected because they have been used for intrusion detection research in the literature for a variety of research fields, such as Construction & Improvement, Internet of Things (IoT), Medical, Network, and Vehicular. The Construction

& Improvement field of research encompasses research that focuses on techniques for improving or building IDSs without seeking to improve a specific area of IDS. The IoT, Medical, Network, and Vehicle research fields include methods that specifically focus improving their respective areas. The metadata for each dataset was compiled into Table I. The following subsections cover the details of each dataset in more depth.

1) *CIC-IDS-2017*: The authors of [36] published CIC-IDS-2017 in 2017. The data was collected by the Canadian Institute for Cybersecurity (CIC) at UNB using two completely separated networks - a Victim-Network and an Attack-Network. A benign-profile (B-profile) was created to imitate human interactions on a network, and six attack profiles were created based on an updated list of common attack families.

2) *CIC-IDS-2018*: Released by CIC in 2018, CIC-IDS-2018 [36] was designed to be an upgraded version of CIC-IDS-2017. The data was collected using two completely separated networks - a Victim-Network and an Attack-Network. A B-profile was created to imitate human interactions on a network, and six attack profiles were used to create malicious traffic.

3) *NSL-KDD*: The University of New Brunswick (UNB) [34] released NSL-KDD in 2009. It was designed as an updated version of KDDCup99 dataset and has four main types of attacks - DoS, U2R, R2L, and Probing.

4) *TON_IoT*: The authors of [37] released TON_IoT in 2019 by UNSW. This dataset was created by UNSW to address the lack of authoritative and representative heterogeneous information for IoT networks. The data was collected from a three layer architecture, which simulated a realistic implementation of recent real-world IoT/Industrial IoT (IIoT) networks - the edge layer, which contained the physical devices and their operating systems; the fog layer, which contained the virtualization technology that programs and controls the VMs; and the cloud layer, which contains the cloud services configured online in the testbed. TON_IoT contains nine types of attacks - Scanning, DoS, DDoS, Ransomware, Backdoor, Injection, XXS, Password Cracking, and Man-In-The-Middle (MITM).

5) *UNSW-NB15*: Created by UNSW and released in 2015 [35], UNSW-NB15 was designed to provide a comprehensive network based dataset. The data was collected from a virtual architecture which consisted of three virtual servers - two normal and one abnormal. This dataset has 197 features and 9 types of attacks - Fuzzers, Analysis, Backdoor, DoS, Exploits, Generic, Reconnaissance, Shellcode, and Worms.

IV. RESULTS

In this section, the results for each set of dataset experiments are provided. As mentioned in Section III, the metrics used to gauge the performance of parHSOM and the Sequential HSOM are precision, recall, F1 score, accuracy, False Positive Rate (FPR), False Negative Rate (FNR), Training Time (TT), and Prediction Time (PT). The result averages for the CIC-IDS-2017 dataset experiments on Testbed 1 and Testbed 2 are displayed in Table II and Table III. CIC-IDS-2017 was

the second largest dataset that was used to test parHSOM. Additionally, it has the lowest contamination rate. The result averages for the CIC-IDS-2018 dataset experiments on Testbed 1 and Testbed 2 are shown in Table IV and Table V. CIC-IDS-2018 was the largest dataset that parHSOM was tested on, and it had the second smallest contamination rate. Table VI and Table VII provide the average results for the NSL-KDD experiments on Testbed 1 and Testbed 2. NSL-KDD was the smallest dataset used to test parHSOM. It has the third smallest contamination rate. The result averages for the TON_IoT dataset experiments on Testbed 1 and Testbed 2 are shown in Table VIII and Table IX. TON_IoT is the second smallest dataset used in this research, and it has the highest contamination rate. Finally, the result averages for the UNSW-NB15 dataset experiments on Testbed 1 and Testbed 2 are displayed in Table X and Table XI. UNSW-NB15 is the third smallest dataset used to test parHSOM, and it has the second highest contamination rate.

A. Speedup Calculations

The speedup for parHSOM was calculated based on the Testbed 1 and Testbed 2 from each dataset's experiment data. The results from each set of experiments were plotted on a bar graph and compared to each other. These comparisons can be found in Figure 2 and Figure 3.

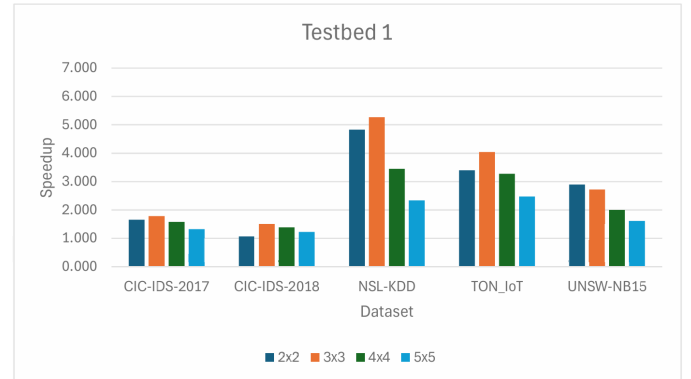


Fig. 2. A figure that compares the speed increase of parHSOM across all of the Testbed 1 experiments.

V. DISCUSSION

As shown in Section III, provides an answer to RQ1, and thus, the focus of the discussion section will be to analyze how the experiment results relate to RQ2.

A. Research Question 2

To understand how parHSOM algorithm compares to the Sequential HSOM algorithm, this research split RQ2 into two subproblems:

- 1) How does the parHSOM Training Time compare to the Sequential HSOM Training Time?

Metadata		Attack Categories							IDS Research Categories				
Datasets	Year	Number of Samples	Contamination Rate	Number of Features	Botnet	Brute Force	DoS / DDoS	Escalation		Infiltration	Injection	Malware	Reconnaissance
NSL-KDD [34]	2009	148,517	48.12%	122	-	-	✓	✓	✓	-	-	✓	Construction & Improvement, IoT, Medical, Network, Vehicular
UNSW-NB15 [35]	2015	257,673	63.91%	197	-	-	✓	✓	✓	-	✓	✓	Construction & Improvement, IoT, Medical, Network, Vehicular
CIC-IDS-2017 [36]	2017	2,827,876	19.68%	78	✓	✓	✓	-	✓	✓	-	✓	Construction & Improvement, Network, Vehicular
CIC-IDS-2018 [36]	2018	7,199,312*	20.60%	81	✓	✓	✓	-	✓	-	-	-	Construction & Improvement
TON-IoT [37]	2019	211,042	76.31%	82	-	✓	✓	-	✓	✓	✓	-	Construction & Improvement, IoT

TABLE I

A TABLE THAT LISTS THE DETAILS OF THE CYBERSECURITY DATASETS USED DURING THE EXPERIMENTS FOR THIS RESEARCH.

CIC-IDS-2017 Dataset: HSOM Training Results							
Testbed 1							
Sequential	Precision		Recall		F1 Score		
	0	1	0	1	0	1	
Grid Size	2x2	0.987	0.907	0.976	0.941	0.980	0.925
	3x3	0.990	0.912	0.978	0.957	0.980	0.932
	4x4	0.989	0.907	0.977	0.948	0.980	0.927
	5x5	0.989	0.897	0.973	0.951	0.980	0.922
parHSOM	Precision		Recall		F1 Score		
	0	1	0	1	0	1	
Grid Size	2x2	0.988	0.914	0.979	0.949	0.981	0.931
	3x3	0.988	0.915	0.979	0.947	0.980	0.930
	4x4	0.986	0.913	0.979	0.944	0.980	0.926
	5x5	0.989	0.897	0.973	0.951	0.980	0.922

Sequential	Accuracy	FPR	FNR	TT (s)	PT (ms)	
	Grid Size	2x2	0.970	0.02358	0.05894	631.314
3x3		0.971	0.02319	0.04342	483.495	0.01194
4x4		0.970	0.02373	0.05312	410.755	0.01307
5x5		0.970	0.02682	0.04893	392.548	0.00989
parHSOM	Accuracy	FPR	FNR	TT (s)	PT (ms)	
	Grid Size	2x2	0.971	0.02166	0.05179	380.789
3x3		0.970	0.02170	0.05424	271.887	0.01314
4x4		0.970	0.02233	0.05732	260.109	0.01080
5x5		0.970	0.02652	0.04942	297.043	0.01073

TABLE II

A TABLE THAT CONTAINS THE RESULT AVERAGES FOR THE EXPERIMENTS CONDUCTED USING THE CIC-IDS-2017 DATASET ON TESTBED 1.

- 2) How do the other parHSOM performance metrics compare to the other Sequential HSOM performance metrics?

RQ2.1 focuses on a central component of this research, which is whether or not parHSOM will train faster than the Sequential HSOM. However, a faster training time is not useful if the trained parHSOM functions significantly worse than the Sequential HSOM in all of the other performance metrics. Thus, RQ2.2 will focus on how the performance metrics of parHSOM compare to the performance metrics of the Sequential HSOM.

1) *Research Question 2 - Subproblem 1:* Analyzing the training time results from the previous sections shows that

CIC-IDS-2017 Dataset: HSOM Training Results (continued)							
Testbed 2							
Sequential	Precision		Recall		F1 Score		
	0	1	0	1	0	1	
Grid Size	2x2	0.987	0.902	0.976	0.942	0.979	0.922
	3x3	0.990	0.905	0.977	0.950	0.980	0.927
	4x4	0.989	0.909	0.979	0.944	0.980	0.928
	5x5	0.990	0.900	0.974	0.950	0.980	0.924
parHSOM	Precision		Recall		F1 Score		
	0	1	0	1	0	1	
Grid Size	2x2	0.987	0.901	0.976	0.944	0.979	0.922
	3x3	0.988	0.915	0.979	0.945	0.980	0.932
	4x4	0.987	0.906	0.977	0.946	0.980	0.926
	5x5	0.989	0.899	0.973	0.949	0.980	0.925

Sequential	Accuracy	FPR	FNR	TT (s)	PT (ms)	
	Grid Size	2x2	0.969	0.02520	0.05692	990.508
3x3		0.970	0.02394	0.05093	815.459	0.02236
4x4		0.970	0.02314	0.05510	701.653	0.02134
5x5		0.970	0.02557	0.04981	713.081	0.02055
parHSOM	Accuracy	FPR	FNR	TT (s)	PT (ms)	
	Grid Size	2x2	0.969	0.02562	0.05679	557.147
3x3		0.971	0.02164	0.05397	431.255	0.02456
4x4		0.970	0.02375	0.05540	460.033	0.02162
5x5		0.970	0.02612	0.04963	540.693	0.02098

TABLE III

A TABLE THAT CONTAINS THE RESULT AVERAGES FOR THE EXPERIMENTS CONDUCTED USING THE CIC-IDS-2017 DATASET ON TESTBED 2.

parHSOM consistently outperformed the Sequential HSOM. However, the amount of speedup achieved by parHSOM changed depending on the experiment variables. The best training time improvement for parHSOM happened when it was trained on the NSL-KDD dataset using the 3x3 grid. With this setup, parHSOM achieved a 5.265 speed increase on Testbed 1 and a 6.056 speed increase on Testbed 2. Further analysis of the other dataset experiments showed similar results. As Table XII shows, parHSOM performed the best using the 3x3 output grid for every set of experiments except for one. The single outlier is when parHSOM was trained on Testbed 1 with the UNSW-NB15 dataset. In that instance, the 2x2 grid size performed the best with a 2.897 speed increase;

CIC-IDS-2018 Dataset: HSOM Training Results							
Testbed 1							
Sequential	Precision		Recall		F1 Score		
	0	1	0	1	0	1	
Grid Size	2x2	0.965	0.962	0.990	0.859	0.980	0.907
	3x3	0.969	0.963	0.990	0.867	0.980	0.911
	4x4	0.967	0.967	0.990	0.863	0.980	0.911
	5x5	0.965	0.953	0.990	0.857	0.978	0.900
parHSOM	Precision		Recall		F1 Score		
	0	1	0	1	0	1	
Grid Size	2x2	0.966	0.964	0.990	0.860	0.978	0.909
	3x3	0.969	0.961	0.990	0.869	0.980	0.915
	4x4	0.964	0.961	0.990	0.858	0.979	0.907
	5x5	0.967	0.951	0.989	0.868	0.980	0.907
Sequential	Accuracy	FPR	FNR	TT (s)	PT (ms)		
Grid Size	2x2	0.965	0.00874	0.13960	1400.726	0.01452	
	3x3	0.969	0.00820	0.13348	1025.441	0.01156	
	4x4	0.967	0.00797	0.13697	949.046	0.00944	
	5x5	0.962	0.01120	0.14379	933.517	0.00966	
parHSOM	Accuracy	FPR	FNR	TT (s)	PT (ms)		
Grid Size	2x2	0.965	0.00868	0.14035	1311.045	0.02177	
	3x3	0.969	0.00864	0.13045	683.330	0.01123	
	4x4	0.962	0.00898	0.14171	685.680	0.01011	
	5x5	0.963	0.01161	0.13261	761.019	0.01097	

TABLE IV

A TABLE THAT CONTAINS THE RESULT AVERAGES FOR THE EXPERIMENTS CONDUCTED USING THE CIC-IDS-2018 DATASET ON TESTBED 1.

CIC-IDS-2018 Dataset: HSOM Training Results (continued)							
Testbed 2							
Sequential	Precision		Recall		F1 Score		
	0	1	0	1	0	1	
Grid Size	2x2	0.966	0.961	0.990	0.859	0.979	0.906
	3x3	0.968	0.965	0.990	0.864	0.980	0.911
	4x4	0.968	0.964	0.990	0.863	0.980	0.909
	5x5	0.968	0.962	0.990	0.863	0.980	0.912
parHSOM	Precision		Recall		F1 Score		
	0	1	0	1	0	1	
Grid Size	2x2	0.965	0.962	0.990	0.860	0.979	0.906
	3x3	0.970	0.963	0.990	0.867	0.980	0.913
	4x4	0.967	0.959	0.989	0.865	0.979	0.908
	5x5	0.965	0.955	0.990	0.862	0.979	0.906
Sequential	Accuracy	FPR	FNR	TT (s)	PT (ms)		
Grid Size	2x2	0.964	0.00905	0.14113	2046.145	0.02127	
	3x3	0.968	0.00804	0.13526	1728.327	0.01945	
	4x4	0.966	0.00853	0.13588	1873.293	0.01924	
	5x5	0.964	0.00882	0.13605	2019.818	0.01976	
parHSOM	Accuracy	FPR	FNR	TT (s)	PT (ms)		
Grid Size	2x2	0.963	0.00877	0.14137	1323.480	0.02353	
	3x3	0.967	0.00853	0.13251	1069.207	0.02193	
	4x4	0.964	0.00974	0.13562	1319.989	0.02000	
	5x5	0.960	0.01069	0.13854	1650.819	0.02122	

TABLE V

A TABLE THAT CONTAINS THE RESULT AVERAGES FOR THE EXPERIMENTS CONDUCTED USING THE CIC-IDS-2018 DATASET ON TESTBED 2.

NSL-KDD Dataset: Training HSOM Results							
Testbed 1							
Sequential	Precision		Recall		F1 Score		
	0	1	0	1	0	1	
Grid Size	2x2	0.968	0.977	0.980	0.962	0.975	0.971
	3x3	0.971	0.976	0.979	0.968	0.976	0.971
	4x4	0.969	0.976	0.979	0.966	0.973	0.971
	5x5	0.969	0.974	0.978	0.967	0.972	0.970
parHSOM	Precision		Recall		F1 Score		
	0	1	0	1	0	1	
Grid Size	2x2	0.964	0.978	0.980	0.959	0.973	0.967
	3x3	0.971	0.976	0.977	0.967	0.972	0.970
	4x4	0.972	0.976	0.978	0.968	0.972	0.971
	5x5	0.970	0.974	0.976	0.968	0.970	0.970
Sequential	Accuracy	FPR	FNR	TT (s)	PT (ms)		
Grid Size	2x2	0.973	0.02107	0.03617	175.390	0.01330	
	3x3	0.975	0.02214	0.03078	143.369	0.01230	
	4x4	0.971	0.02305	0.03354	87.055	0.01192	
	5x5	0.970	0.02377	0.03269	67.400	0.01140	
parHSOM	Accuracy	FPR	FNR	TT (s)	PT (ms)		
Grid Size	2x2	0.972	0.02081	0.04111	36.300	0.01490	
	3x3	0.972	0.02304	0.03296	27.229	0.01256	
	4x4	0.972	0.02273	0.03209	25.232	0.01125	
	5x5	0.970	0.02368	0.03273	28.832	0.01254	

TABLE VI

A TABLE THAT CONTAINS THE RESULT AVERAGES FOR THE EXPERIMENTS CONDUCTED USING THE NSL-KDD DATASET ON TESTBED 1.

NSL-KDD Dataset: HSOM Training Results (continued)							
Testbed 2							
Sequential	Precision		Recall		F1 Score		
	0	1	0	1	0	1	
Grid Size	2x2	0.969	0.977	0.978	0.962	0.974	0.969
	3x3	0.971	0.977	0.979	0.969	0.973	0.971
	4x4	0.967	0.976	0.977	0.965	0.970	0.970
	5x5	0.968	0.974	0.976	0.966	0.971	0.970
parHSOM	Precision		Recall		F1 Score		
	0	1	0	1	0	1	
Grid Size	2x2	0.967	0.978	0.980	0.964	0.973	0.970
	3x3	0.972	0.977	0.978	0.970	0.975	0.970
	4x4	0.970	0.976	0.977	0.967	0.971	0.970
	5x5	0.971	0.972	0.977	0.969	0.971	0.970
Sequential	Accuracy	FPR	FNR	TT (s)	PT (ms)		
Grid Size	2x2	0.972	0.02167	0.03695	305.143	0.02294	
	3x3	0.973	0.02283	0.03170	247.008	0.02127	
	4x4	0.970	0.02242	0.03568	153.109	0.02127	
	5x5	0.970	0.02350	0.03468	116.323	0.02172	
parHSOM	Accuracy	FPR	FNR	TT (s)	PT (ms)		
Grid Size	2x2	0.972	0.02169	0.03670	73.174	0.02372	
	3x3	0.972	0.02260	0.03027	40.788	0.02127	
	4x4	0.970	0.02336	0.03376	35.023	0.02153	
	5x5	0.970	0.02391	0.03182	43.685	0.02220	

TABLE VII

A TABLE THAT CONTAINS THE RESULT AVERAGES FOR THE EXPERIMENTS CONDUCTED USING THE NSL-KDD DATASET ON TESTBED 2.

TON_IoT Dataset: HSOM Training Results

Testbed 1							
Sequential	Precision		Recall		F1 Score		
	0	1	0	1	0	1	
Grid Size	2x2	0.938	0.974	0.918	0.981	0.927	0.976
	3x3	0.951	0.983	0.942	0.986	0.946	0.985
	4x4	0.956	0.984	0.944	0.987	0.950	0.987
	5x5	0.961	0.977	0.923	0.988	0.940	0.983
parHSOM		Precision		Recall		F1 Score	
		0	1	0	1	0	1
Grid Size	2x2	0.965	0.977	0.931	0.989	0.946	0.984
	3x3	0.946	0.985	0.948	0.983	0.946	0.983
	4x4	0.952	0.986	0.954	0.987	0.952	0.986
	5x5	0.955	0.978	0.930	0.987	0.941	0.982

Sequential	Accuracy	FPR	FNR	TT (s)	PT (ms)	
Grid Size	2x2	0.965	0.08249	0.01948	111.904	0.00958
	3x3	0.973	0.05760	0.01504	104.861	0.00956
	4x4	0.976	0.05557	0.01348	86.247	0.00978
	5x5	0.973	0.07771	0.01223	70.049	0.01104
parHSOM		Accuracy	FPR	FNR	TT (s)	PT (ms)
Grid Size	2x2	0.976	0.06877	0.01094	32.894	0.01068
	3x3	0.973	0.05294	0.01707	25.953	0.00980
	4x4	0.979	0.04694	0.01473	26.326	0.00994
	5x5	0.972	0.06975	0.01429	28.315	0.01042

TABLE VIII

A TABLE THAT CONTAINS THE RESULT AVERAGES FOR THE EXPERIMENTS CONDUCTED USING THE TON_IoT DATASET ON TESTBED 1.

UNSW-NB15 Dataset: HSOM Training Results

Testbed 1							
Sequential	Precision		Recall		F1 Score		
	0	1	0	1	0	1	
Grid Size	2x2	0.899	0.932	0.881	0.944	0.889	0.940
	3x3	0.894	0.927	0.870	0.940	0.883	0.936
	4x4	0.886	0.928	0.871	0.936	0.879	0.930
	5x5	0.917	0.910	0.836	0.957	0.871	0.931
parHSOM		Precision		Recall		F1 Score	
		0	1	0	1	0	1
Grid Size	2x2	0.895	0.932	0.877	0.944	0.887	0.938
	3x3	0.895	0.928	0.867	0.941	0.879	0.933
	4x4	0.885	0.928	0.873	0.936	0.879	0.930
	5x5	0.923	0.904	0.820	0.962	0.869	0.930

Sequential	Accuracy	FPR	FNR	TT (s)	PT (ms)	
Grid Size	2x2	0.920	0.12065	0.05599	285.993	0.01843
	3x3	0.917	0.12894	0.05767	196.958	0.01523
	4x4	0.911	0.12864	0.06325	147.377	0.01309
	5x5	0.911	0.16647	0.04373	140.881	0.01268
parHSOM		Accuracy	FPR	FNR	TT (s)	PT (ms)
Grid Size	2x2	0.919	0.12332	0.05762	98.718	0.02351
	3x3	0.916	0.13197	0.05874	72.431	0.01309
	4x4	0.912	0.12680	0.06423	73.804	0.01190
	5x5	0.910	0.18163	0.03920	87.161	0.01221

TABLE X

A TABLE THAT CONTAINS THE RESULT AVERAGES FOR THE EXPERIMENTS CONDUCTED USING THE UNSW-NB15 DATASET ON TESTBED 1.

TON_IoT Dataset: HSOM Training Results (continued)

Testbed 2							
Sequential	Precision		Recall		F1 Score		
	0	1	0	1	0	1	
Grid Size	2x2	0.941	0.973	0.914	0.982	0.927	0.976
	3x3	0.956	0.986	0.946	0.988	0.950	0.985
	4x4	0.952	0.986	0.955	0.985	0.955	0.986
	5x5	0.957	0.980	0.939	0.988	0.948	0.984
parHSOM		Precision		Recall		F1 Score	
		0	1	0	1	0	1
Grid Size	2x2	0.919	0.979	0.928	0.974	0.922	0.976
	3x3	0.959	0.987	0.949	0.989	0.953	0.987
	4x4	0.956	0.987	0.953	0.988	0.955	0.987
	5x5	0.956	0.979	0.932	0.987	0.944	0.983

Sequential	Accuracy	FPR	FNR	TT (s)	PT (ms)	
Grid Size	2x2	0.966	0.08565	0.01766	186.640	0.01998
	3x3	0.976	0.05514	0.01372	191.626	0.01972
	4x4	0.979	0.04461	0.01495	150.120	0.01924
	5x5	0.975	0.06058	0.01326	129.202	0.02053
parHSOM		Accuracy	FPR	FNR	TT (s)	PT (ms)
Grid Size	2x2	0.964	0.07098	0.02591	50.347	0.02005
	3x3	0.978	0.05002	0.01263	40.475	0.02041
	4x4	0.980	0.04719	0.01353	43.918	0.02010
	5x5	0.973	0.06764	0.01369	52.755	0.02203

TABLE IX

A TABLE THAT CONTAINS THE RESULT AVERAGES FOR THE EXPERIMENTS CONDUCTED USING THE TON_IoT DATASET ON TESTBED 2.

UNSW-NB15 Dataset: HSOM Training Results (continued)

Testbed 2							
Sequential	Precision		Recall		F1 Score		
	0	1	0	1	0	1	
Grid Size	2x2	0.898	0.930	0.875	0.946	0.887	0.938
	3x3	0.896	0.927	0.871	0.942	0.885	0.937
	4x4	0.884	0.929	0.873	0.935	0.880	0.930
	5x5	0.932	0.899	0.809	0.966	0.865	0.931
parHSOM		Precision		Recall		F1 Score	
		0	1	0	1	0	1
Grid Size	2x2	0.897	0.929	0.874	0.944	0.887	0.938
	3x3	0.893	0.929	0.871	0.940	0.882	0.936
	4x4	0.886	0.925	0.866	0.940	0.877	0.930
	5x5	0.923	0.903	0.819	0.961	0.868	0.931

Sequential	Accuracy	FPR	FNR	TT (s)	PT (ms)	
Grid Size	2x2	0.920	0.12424	0.05512	447.686	0.02379
	3x3	0.917	0.12951	0.05713	319.229	0.02298
	4x4	0.911	0.12473	0.06506	198.260	0.02153
	5x5	0.910	0.19137	0.03436	180.196	0.02344
parHSOM		Accuracy	FPR	FNR	TT (s)	PT (ms)
Grid Size	2x2	0.919	0.12509	0.05638	176.467	0.02565
	3x3	0.916	0.12872	0.05918	87.013	0.02582
	4x4	0.912	0.13327	0.06146	74.787	0.02229
	5x5	0.911	0.18152	0.03838	85.453	0.02367

TABLE XI

A TABLE THAT CONTAINS THE RESULT AVERAGES FOR THE EXPERIMENTS CONDUCTED USING THE UNSW-NB15 DATASET ON TESTBED 2.

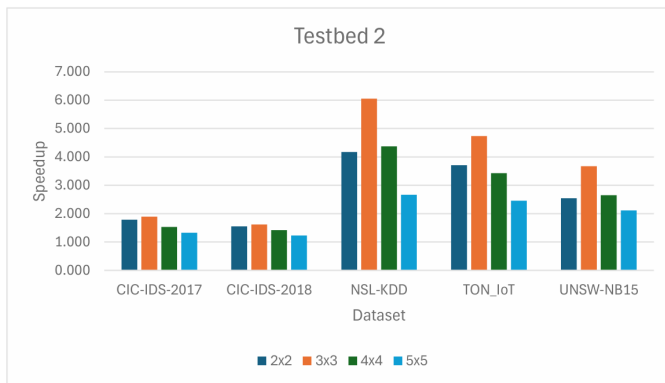


Fig. 3. A figure that compares the speed increase of parHSOM across all of the Testbed 2 experiments.

	Best parHSOM Training Time Results			
	Speedup	Grid Size	Testbed 1	Testbed 2
CIC-IDS-2017	1.778	3x3	X	-
	1.891	3x3	-	X
CIC-IDS-2018	1.501	3x3	X	-
	1.616	3x3	-	X
NSL-KDD	5.265	3x3	X	-
	6.056	3x3	-	X
TON_IoT	4.04	3x3	X	-
	4.734	3x3	-	X
UNSW-NB15	2.897	2x2	X	-
	3.669	3x3	-	X

TABLE XII

A TABLE THAT SHOWS THE CONDITIONS FOR PARHSOM'S GREATEST SPEED INCREASE IN EACH OF THE DATASET EXPERIMENTS.

however, even in that case, the 2x2 output grid only narrowly beat the 3x3 grid, which had a 2.719 speed increase. These observations imply that parHSOM performs best using a 3x3 grid.

Another trend this work observed in the training time results was that as the size of the dataset increased, the amount of parHSOM speedup decreased. Since the number of spawned child processes also increases with the size of the dataset, this would imply that as the size of the dataset increases the CPU becomes overloaded with children processes.

While the experiments on Testbed 1 consistently finished training faster than the Testbed 2 experiments, the Testbed 2 experiments showed higher speed increase between parHSOM and the Sequential HSOM. The slower train times on Testbed 2 would imply overhead communication costs between the two sockets. However, the higher speedup implies room for improvement if the socket communication can be optimized.

2) *Research Question 2 - Subproblem 2*: To assess how parHSOM performed in comparison to the Sequential HSOM, this work calculated the difference between the performance of parHSOM and the Sequential HSOM for all of our experiments. For the CIC-IDS-2017, CIC-IDS-2018, and NSL-KDD experiments, all of the respective performance values were within 0.01 of each other, and for the TON_IoT and UNSW-NB15 experiments, most of the respective performance values were within 0.01 of each other with

a couple of the values being within 0.03 of each. Thus, it can be concluded that no significant change occurred in the precision, recall, F1score, accuracy, FPR, FNR, or PT between the Sequential HSOM and parHSOM. This point is further emphasized when the accuracy, False Positive Rate (FPR), and False Negative Rate (FNR) performance metrics are examined in greater detail. To analyze them further, each group of metrics was converted to percentages and graphed.

Accuracy Metrics: First, the accuracy metrics were converted to percentages, and then, the percentages were graphed to compare the outcomes from each of the dataset experiments. In the CIC-IDS-2017 experiments, all of the accuracy metrics were within 0.2% of each other, and parHSOM performed the best on Testbed 1 with a 2x2 grid and on Testbed 2 with a 3x3 grid. For CIC-IDS-2018, the accuracy metrics were within 0.9% of each other, and parHSOM performed the best on both Testbed 1 and Testbed 2 with a 3x3 grid. In the NSL-KDD experiments, the accuracy range from 97.00% to 97.50%, which results in a difference of 0.5%. parHSOM had the same level of accuracy for each of the grid sizes on Testbed 1, and it performed the best on Testbed 2 with both the 2x2 and 3x3 grid. The TON_IoT experiments showed the largest difference between the accuracy metrics for this research with a range of 1.6%; however, for each of the different grid sizes, parHSOM performed better than or very similar to the Sequential HSOM. parHSOM performed the best on both Testbed 1 and Testbed 2 with the 4x4 grid. However, it is interesting to note that the largest difference between the Sequential HSOM and parHSOM was for the 2x2 grid experiments where parHSOM performed better than the Sequential HSOM by 1%. Finally for UNSW-NB15, the accuracy metrics were within 1.0% of each other, and parHSOM performed the best on both Testbed 1 and Testbed 2 with the 2x2 grid.

False Positive Rate (FPR) Metrics: Similar to the accuracy metrics, the FPR metrics were converted into percentages and graphed in order to analyze the difference between parHSOM and the Sequential HSOM. For CIC-IDS-2017, the FPR metrics ranged from 2.16% to 2.68%, which results in a difference of 0.52%. parHSOM performed the best on Testbed 1 with the 2x2 and 3x3 grid and on Testbed 2 with the 3x3 grid. In the CIC-IDS-2018 experiments, all of the FPR metrics were within 0.36% of each other, and parHSOM performed the best on both Testbed 1 and Testbed 2 with the 3x3 grid. The NSL-KDD experiments presented FPR metrics that were within 0.31% of each other, and parHSOM performed the best on both Testbed 1 and Testbed 2 with the 2x2 grid. The TON_IoT experiments showed a larger split with the percentages ranging from 4.46% to 8.57%, for a difference of 4.11%. However, parHSOM performed better than the Sequential HSOM for all grid sizes except the 5x5 grid on Testbed 2, and in that case, parHSOM only differed from the Sequential HSOM by 0.70%. parHSOM performed the best on both Testbed 1 and Testbed 2 with the 4x4 grid size. Finally, in the UNSW-NB15 experiments, this research recorded the largest gap of percentages, with a range of 7.07%. However, the larger percentage range is due to the

different grid sizes producing different results. Within the same grid size, parHSOM performed similar to, if not better than, the Sequential HSOM. parHSOM performed the best on both Testbed 1 and Testbed 2 with the 2x2 grid.

False Negative Rate (FNR) Metrics: Like the previous section, the False Negative Metrics were converted into percentages and then graphed in order to analyze how parHSOM compared to the Sequential HSOM. In the CIC-IDS-2017 experiments, all of the FNR metrics were within 1.55% of each other. Analyzing the metrics showed that the largest gap between the Sequential HSOM and parHSOM was in the experiments using the 3x3 grid size on Testbed 1. However, even then, the models only differed by 1.08%. In all other cases, the difference between the Sequential HSOM and parHSOM was less than 0.5%, and for the 2x2 grid experiments on Testbed 1, parHSOM outperformed the Sequential HSOM. parHSOM performed the best on both Testbed 1 and Testbed 2 with the 5x5 grid. The CIC-IDS-2018 experiments showed FNR metrics that were within 1.33% of each other. This range comes from the various grid sizes performing differently. In all cases, the difference between parHSOM and the Sequential HSOM was less than 0.5%, in most of the cases, parHSOM differed from the Sequential HSOM by less than 0.25%, and in four of the cases, parHSOM performed better than the Sequential HSOM. parHSOM performed best on both Testbed 1 and Testbed 2 with the 3x3 grid. In the NSL-KDD experiments, the FNR metrics ranged from 3.08% to 4.11%. In all cases, parHSOM differed from the Sequential HSOM by less than 0.5%, and in five out of the eight experiment setups, parHSOM performed better than the Sequential HSOM. parHSOM performed the best on both Testbed 1 and Testbed 2 with the 3x3 grid. In the TON_IoT experiments, the FNR metrics ranged from 1.26% to 8.25%. The experiments on Testbed 1 resulted in consistently higher FNRs. However, in each case, parHSOM performed better than the Sequential HSOM. The experiments run on Testbed 2 consistently returned lower FNRs. Within those results, parHSOM performed better than the Sequential HSOM on the 3x3 and 4x4 grid sizes, very similar on the 5x5 grid, and less than 1% different on the 2x2 grid. parHSOM performed best on Testbed 1 with the 4x4 grid and on Testbed 2 with the 3x3 grid. Finally, for UNSW-NB15, the FNR metrics are all within 3.07% of each other. The experiments run using the 5x5 grid size performed better than the other grid sizes, and thus, increased the range of FNR metric percentages. parHSOM performed the best on both Testbed 1 and Testbed 2 with the 5x5 grid.

VI. CONCLUSION

This research set out to design a parallel HSOM implementation. After researching various parallelization methods for the SOM, this work proposed the parHSOM algorithm. parHSOM is based on the data-partitioned parallelization method, and it has been tested on two different environments, four different grid sizes, and five different cybersecurity datasets. Using the experiment data, this research answered

two research questions. RQ1 focused solely on whether or not parallelizing the HSOM was possible and was answered in Section III. RQ2 focused on how parHSOM performed compared to the Sequential HSOM. In Section IV, this work divided RQ2 into two subproblems. The first subproblem focused on the Training Time of parHSOM, while the second subproblem focused on the other performance metrics of parHSOM. In subproblem 1, this work showed that parHSOM consistently performed better than the Sequential HSOM, with a maximum speed increase of 6.056. Analyzing the other performance metrics provided an answer to subproblem 2, where this work showed that parHSOM performed similarly, if not better than, the Sequential HSOM. Overall, these experiments have shown that parHSOM contains potential as a parallel HSOM implementation. In the next section, this work covers some of the limitations of this research and how those limitations link to areas of future research.

A. Limitations

Due to the lack of literature on parallel HSOM implementations, this work started with the base level components of the HSOM algorithm and analyzed what happened when those base components were parallelized using the data-partitioned method. However, this research was not without its limitations. First, while the HSOM algorithm was designed to mitigate the SOM algorithm's sensitivity to initial conditions, the HSOM is not immune to this weakness. This work standardized all of the initial conditions, such as the learning rate and neighborhood function, except for the output grid size which was limited to four specific sizes. This decision was made so that the effect of parallelizing the HSOM could be better observed due to the reduced amount of changing factors. However, as the size of the weight updates decreased, the model sent Runtime error messages indicating that the initialization factors could be better optimized. Another limitation of this work is the fact that parHSOM was designed using Python. Python was chosen to help provide a starting point for parallel HSOM research, but it is not the optimal programming language for reducing communication overhead. Instead of being drawbacks, these limitations provide insight into future areas of research, which will be discussed in the next section.

B. Future Work

parHSOM shows that there is potential in parallelizing the HSOM algorithm. One area of future research would be to analyze what happens if parHSOM is implemented in a more efficient programming language, such as MPI. With this language, researchers could investigate whether or not the communication overhead of parHSOM can be decreased. Another area of future research would be to investigate how initialization parameters affect parHSOM's performance. parHSOM could be expanded into a Growing Hierarchical Self-Organizing Map (GHSOM), which has been shown in the literature to help further reduce the SOM algorithm's sensitivity to initial conditions. Finally, a third area of future

research would be to investigate how parHSOM performs if it was modified to utilize GPU resources.

In conclusion, this research provides a starting point for parallel implementations of the HSOM algorithm. Furthermore, it highlights areas of future research. Finally, it demonstrates that parallelizing the HSOM algorithm is a promising field of research for improving explainable, trustworthy, and AI-based IDSs.

VII. ACKNOWLEDGMENTS

The authors would like to acknowledge the support of the Predictive Analytics and Technology Integration (PATENT) Laboratory for their support regarding finances, technology, and leadership in this work.

REFERENCES

- [1] J. Ables, T. Kirby, W. Anderson, S. Mittal, S. Rahimi, I. Banicescu, and M. Seale, "Creating an explainable intrusion detection system using self organizing maps," in *2022 IEEE Symposium Series on Computational Intelligence (SSCI)*. IEEE, 2022, pp. 404–412.
- [2] F. Cuello, "Self-organizing maps," 2024, website Title: TrednSpider Learning Center. [Online]. Available: <https://trendspider.com/learning-center/self-organizing-maps/>
- [3] A. Panwar and S. J. Nanda, "Data analysis in wireless sensor networks with distributed self organizing map," in *2024 IEEE 1st International Conference on Advances in Signal Processing, Power, Communication, and Computing (ASPCC)*, 2024, pp. 61–66.
- [4] K. Bagher, I. Khalil, A. Alabdulatif, and M. Atiquzzaman, "Edgesom: Distributed hierarchical edge-driven iot data analytics framework," *Computer Communications*, vol. 172, pp. 64–74, 2021. [Online]. Available: <https://www.sciencedirect.com/science/article/pii/S0140366421000906>
- [5] A. De, Y. Zhang, and C. Guo, "A parallel adaptive segmentation method based on som and gpu with application to mri image processing," *Neurocomputing*, vol. 198, pp. 180–189, 2016, advances in Neural Networks, Intelligent Control and Information Processing. [Online]. Available: <https://www.sciencedirect.com/science/article/pii/S0925231216003283>
- [6] T. Kohonen, "The self-organizing map," *Proceedings of the IEEE*, vol. 78, no. 9, pp. 1464–1480, 1990.
- [7] R. Mancini, A. Ritacco, G. Lanciano, and T. Cucinotta, "Xpysom: High-performance self-organizing maps," in *2020 IEEE 32nd International Symposium on Computer Architecture and High Performance Computing (SBAC-PAD)*, 2020, pp. 209–216.
- [8] B. Cui, J.-C. Créput, and L. Zhang, "Self-organizing maps and full gpu parallel approach to graph matching," *Computer Communications*, vol. 198, pp. 217–227, 2023. [Online]. Available: <https://www.sciencedirect.com/science/article/pii/S0140366422004558>
- [9] S. Ghorpade and G. Bruns, "A tutorial on self-organizing maps," California State University, 2023.
- [10] T. V. Phan, N. K. Bao, and M. Park, "Distributed-som: A novel performance bottleneck handler for large-sized software-defined networks under flooding attacks," *Journal of Network and Computer Applications*, vol. 91, pp. 14–25, 2017. [Online]. Available: <https://www.sciencedirect.com/science/article/pii/S1084804517301649>
- [11] M. Kim, S. Jung, and M. Park, "A distributed self-organizing map for dos attack detection," in *2015 Seventh International Conference on Ubiquitous and Future Networks*, 2015, pp. 19–22.
- [12] B. L. Vrusias, L. Vomvoridis, and L. Gillam, "Distributing som ensemble training using grid middleware," in *2007 International Joint Conference on Neural Networks*, 2007, pp. 2712–2717.
- [13] F. L. Gorgonio and J. A. F. Costa, "Parallel self-organizing maps with application in clustering distributed data," in *2008 IEEE International Joint Conference on Neural Networks (IEEE World Congress on Computational Intelligence)*, 2008, pp. 3276–3283.
- [14] F. Gorgonio and J. Costa, "Combining parallel self-organizing maps and k-means to cluster distributed data," in *2008 11th IEEE International Conference on Computational Science and Engineering - Workshops*, 2008, pp. 53–58.
- [15] M. Jayaratne, D. Alahakoon, D. De Silva, and X. Yu, "Apache spark based distributed self-organizing map algorithm for sensor data analysis," in *IECON 2017 - 43rd Annual Conference of the IEEE Industrial Electronics Society*, 2017, pp. 8343–8349.
- [16] M. Jayaratne, D. Alahakoon, and D. de Silva, "Unsupervised skill transfer learning for autonomous robots using distributed growing self organizing maps," *Robotics and Autonomous Systems*, vol. 144, p. 103835, 2021. [Online]. Available: <https://www.sciencedirect.com/science/article/pii/S0921889021001202>
- [17] J. Hammond, D. MacClean, and I. Valova, "A parallel implementation of a growing som promoting independent neural networks over distributed input space," in *The 2006 IEEE International Joint Conference on Neural Network Proceedings*, 2006, pp. 958–965.
- [18] P. Ozdzyński, A. Lin, M. Liljeholm, and J. Beatty, "A parallel general implementation of kohonen's self-organizing map algorithm: performance and scalability," *Neurocomputing*, vol. 44–46, pp. 567–571, 2002, computational Neuroscience Trends in Research 2002. [Online]. Available: <https://www.sciencedirect.com/science/article/pii/S0925231202004277>
- [19] A. Rauber, P. Tomsich, and D. Merkl, "parsom: a parallel implementation of the self-organizing map exploiting cache effects: making the som fit for interactive high-performance data analysis," in *Proceedings of the IEEE-INNS-ENNS International Joint Conference on Neural Networks. IJCNN 2000. Neural Computing: New Challenges and Perspectives for the New Millennium*, vol. 6, 2000, pp. 177–182 vol.6.
- [20] N. Bandeira, V. Lobo, and F. Moura-Pires, "Training a self-organizing map distributed on a pvm network," in *1998 IEEE International Joint Conference on Neural Networks Proceedings. IEEE World Congress on Computational Intelligence (Cat. No.98CH36227)*, vol. 1, 1998, pp. 457–461 vol.1.
- [21] H. Guan, C. kwong Li, T. yat Cheung, and S. Yu, "Parallel design and implementation of som neural computing model in pvm environment of a distributed system," in *Proceedings. Advances in Parallel and Distributed Computing*, 1997, pp. 26–31.
- [22] G. Myklebust and J. Solheim, "Parallel self-organizing maps for actual applications," in *Proceedings of ICNN'95 - International Conference on Neural Networks*, vol. 2, 1995, pp. 1054–1059 vol.2.
- [23] T. Hämmäläinen, H. Klapuri, J. Saarinen, and K. Kaski, "Mapping of som and lvq algorithms on a tree shape parallel computer system," *Parallel Computing*, vol. 23, no. 3, pp. 271–289, 1997. [Online]. Available: <https://www.sciencedirect.com/science/article/pii/S0167819197000203>
- [24] L. Vojtěšek, J. Dvorský, K. Slaninová, and J. Martinovič, "Scalable parallel som learning for web user profiles," in *2013 13th International Conference on Intelligent Systems Design and Applications*, 2013, pp. 283–288.
- [25] L.-C. Chang and F.-J. Chang, "An efficient parallel algorithm for lissom neural network," *Parallel Computing*, vol. 28, no. 11, pp. 1611–1633, 2002. [Online]. Available: <https://www.sciencedirect.com/science/article/pii/S0167819102001667>
- [26] L. Zhu, W. Guo, and Y. Bai, "Self-organizing maps neural networks on parallel cluster," in *2009 First International Conference on Information Science and Engineering*, 2009, pp. 384–388.
- [27] S. Q. Khan and M. A. Ismail, "Design and implementation of parallel som model on gpgpu," in *2013 5th International Conference on Computer Science and Information Technology*, 2013, pp. 233–237.
- [28] F. C. Moraes, S. C. Botelho, N. D. Filho, and J. F. O. Gaya, "Parallel high dimensional self organizing maps using cuda," in *2012 Brazilian Robotics Symposium and Latin American Robotics Symposium*, 2012, pp. 302–306.
- [29] W. Qu, F. Bashir, D. Graupe, A. Khokhar, and D. Schonfeld, "A motion trajectory based video retrieval system using parallel adaptive self organizing maps," in *Proceedings. 2005 IEEE International Joint Conference on Neural Networks, 2005.*, vol. 3, 2005, pp. 1800–1805 vol. 3.
- [30] H. Wang, A. Mansouri, and J.-C. Créput, "Massively parallel cellular matrix model for self-organizing map applications," in *2015 IEEE International Conference on Electronics, Circuits, and Systems (ICECS)*, 2015, pp. 584–587.
- [31] T. Richardson and E. Winer, "Extending parallelization of the self-organizing map by combining data and network partitioned methods," *Advances in Engineering Software*, vol. 88, pp. 1–7, 2015. [Online]. Available: <https://www.sciencedirect.com/science/article/pii/S0965997815000769>

- [32] M.-H. Yang and N. Ahuja, "A data partition method for parallel self-organizing map," in *IJCNN'99. International Joint Conference on Neural Networks. Proceedings (Cat. No.99CH36339)*, vol. 3, 1999, pp. 1929–1933 vol.3.
- [33] J. Ables, T. Kirby, S. Mittal, I. Banicescu, S. Rahimi, W. Anderson, and M. Seale, "Explainable intrusion detection systems using competitive learning techniques," *arXiv preprint arXiv:2303.17387*, 2023.
- [34] M. Tavallae, E. Bagheri, W. Lu, and A. A. Ghorbani, "A detailed analysis of the kdd cup 99 data set," in *2009 IEEE symposium on computational intelligence for security and defense applications*. Ieee, 2009, pp. 1–6.
- [35] N. Moustafa and J. Slay, "Unsw-nb15: a comprehensive data set for network intrusion detection systems (unsw-nb15 network data set)," in *2015 military communications and information systems conference (MilCIS)*. IEEE, 2015, pp. 1–6.
- [36] I. Sharafaldin, A. H. Lashkari, A. A. Ghorbani *et al.*, "Toward generating a new intrusion detection dataset and intrusion traffic characterization." *ICISSp*, vol. 1, pp. 108–116, 2018.
- [37] N. Moustafa, "A new distributed architecture for evaluating ai-based security systems at the edge: network ton_iot datasets. sustain. cities soc. 72, 102994 (2021)," 2021.